Temperature-Dependent Electromagnetic Surface Wave Supported by Graphene-Loaded Indium Antimonide Planar Structure

Hindawi
International Journal of Optics
Volume 2024, Article ID 9607121, 10 pages
https://doi.org/10.1155/2024/9607121

Research Article

Temperature-Dependent Electromagnetic Surface Wave Supported by Graphene-Loaded Indium Antimonide Planar Structure

M. Z. Yaqoob,[1] **Ahtisham Ali**,[1] **Majeed A. S. Alkanhal**,[2] **A. Ghaffar**,[3] **Y. Khan**,[2] **and M. Umair**[4]

[1]*Department of Physics, Government College University, Faisalabad 38000, Pakistan*
[2]*Department of Electrical Engineering, King Saud University, Riyadh, Saudi Arabia*
[3]*Department of Physics, University of Agriculture, Faisalabad 38000, Pakistan*
[4]*School of Electrical Engineering and Computer Science, Pennsylvania State University, State College, PA, USA*

Correspondence should be addressed to A. Ghaffar; aghaffar16@uaf.edu.pk

Received 10 October 2023; Revised 20 December 2023; Accepted 23 December 2023; Published 5 January 2024

Academic Editor: Nicola Curreli

In this study, the propagation characteristics of EM surface waves supported by the graphene-coated indium antimonide (InSb) planar waveguide have been investigated theoretically and numerically. The modeling of graphene has been performed by use of Kubo formalism whereas the relative permittivity of indium antimonide has been calculated using Drude's model. The results for transverse electric (TE) and transverse magnetic (TM) polarized surface waves have been computed analytically and numerically. The major challenge is to model the atomically thick graphene sheet over the InSb grounded slab. To get the temperature-dependent characteristic equation for the electromagnetic surface waves, the surface current boundary conditions' approach has been employed. The numerical results have been computed for both the TE and TM polarization states and reported that the TE does not support the propagation of surface waves. The dispersion relation, effective mode index, phase speed, propagation length, and field profile have been computed in Mathematica under TM polarization. The graphene and indium antimonide have been found active for low and high Terahertz regions, respectively. As temperature increases, the plasma frequency of the InSb increases due to this reason with the increase of temperature and the resonance frequency, leading to a shift in the dispersion curve. Moreover, with the increase of temperature, the effective wave number of transverse magnetic polarized surface waves also increases. Resultantly, the confinement of such surface waves supported by graphene-loaded InSb increases. It is shown that with the variation of temperature of indium antimonide, the surface waves propagating across the interface can be tuned in the Terahertz region and can be exploited for thermo-optical sensing, near-field communications waveguides, and graphene-based temperature sensor designing.

1. Introduction

In recent years, the study of surface waves has attracted significant attention due to their potential applications in a wide range of fields, including sensing, imaging, waveguides, filters, modulators, and surface communications [1–8]. Electromagnetic surface waves (ESWs) propagate along the interface between two media, and they can be confined and manipulated at the nanoscale using plasmonic structures. Depending upon the types of partnering surfaces, different types of ESWs can be induced. The ESWs which are controlled by the interface of a metal and any dielectric material having components of polaritons called surface plasmons-polaritons (SPPs) [9, 10]. The EM surface waves are guided by the interfaces of two partnering materials, one with isotropic and other anisotropic dielectric in nature, that type of wave is called Dyakonov surface waves [11]. The electromagnetic surface wave propagation in which at least one of the two interacting materials is often non-homogenous is perpendicular to the interface guiding

surface waves and both interacting materials are isotropic dielectric in nature. That particular type of surface wave is called the Tamm wave [11]. The interfaces of two dielectric materials, where one dielectric material is jointly anisotropic and periodically nonhomogenous in a direction perpendicular to the interface, guide a Dyakonov–Tamm wave, combining the features of Dyakonov wave and Tamm wave. The nonhomogenous electromagnetic surface wave is called the Zenneck or Sommerfeld–Zenneck wave which is incident onto a spherical or planar boundary interface with a complex Brewster angle between two homogeneous media with different dielectric constants [12–14]. Electromagnetic surface waves offer efficient and low-loss transmission of information over short distances, along with light confinement in small spaces, making them valuable for compact optical devices such as sensors, filters, and waveguides [15]. Different types of schemes have been proposed by many researchers to control and manipulate the electromagnetic waves of different spectral ranges, i.e., metastructures, near-zero-index materials, and nanostructures [16–18]. For the visible range, the different plasmonic platforms have been studied for strong interaction with biomolecules and nanostructures and holding potential for applications such as biosensing, drug delivery, waveguides, and nanophotonic [19–21].

To control the THz waves for the surface communication, biomedical sensing, DNA detection, THz antenna, filters, and absorbers, graphene has been realized as a natural metasurface [22–25]. Graphene is a monoatomic, transparent sheet of carbon with its exceptional optical, thermal, electrical, and mechanical properties [26]. Graphene, as proposed by Vakil and Engheta, holds immense promise as a material for actively tuning surface waves with unparalleled control. This potential opens up exciting opportunities for applications in surface communication, cloaking, and sensing [27]. Naserpour et al. theoretically proposed the active tunability and cloaking for the graphene-coated nanodimmers and nanowires [28]. Recently, the graphene-based THz metamaterials have been studied for the promising applications, i.e., biosensing, enhanced light emission, and broadband IR photodetector [29–32]. The exceptional properties of graphene make it a potential candidate for its unprecedented control and manipulation in Terahertz region. Recently, the graphene-based temperature-assisted devices are the interest of many researchers for their potential applications in the wearable temperature sensors, thermographers, thermal current generation, thermal rectifiers, and IR detectors [33–35]. The temperature-sensitive materials (TSM) have temperature-dependent optical, electronic, structural, and phase characteristics; i.e., with the change of external temperature, the characteristics of TSM can be tailored [36]. Indium antimonide (InSb) is realized as temperature-sensitive materials, which electronically has the characteristic of semiconductors formed by the combination of indium (In) and antimony (Sb). Due to its small bandgap, indium antimonide (InSb) growth has received interest as a possible material for infrared detectors and high-speed devices in recent years [37]. InSb-based biosensors can be used to detect microorganisms and are used in temperature-dependent imaging cameras [38]. The response of the graphene towards the thermal agitation is negligible to develop the highly sensitive graphene-based thermal platforms for the communication and sensors, a graphene-loaded indium antimonide (InSb) as a temperature-sensitive material (TSM) has been proposed in the present study. As the surface waves propagate along the interface of two dissimilar media and are sensitive to the electromagnetic characteristics of patterning material, therefore, it is hypothesized that by making an interface of temperature sensitivity, the characteristics of surface may be controlled by the external temperature. Moreover, to tune the surface waves supported by InSb is the biggest challenge and need for the realization of the TSM-based devices. To meet this need, the graphene-coated InSb planar structure has been studied analytically and numerically for the active tuning and manipulation of surface waves from lower to higher THz region. The temperature dependency and effect of graphene parameters on the dispersion curves, effective wave number, and field profiles of surface waves have been studied for both transverse electric (TE) and transverse magnetic (TM) polarizations. The organization of the manuscript is given as the analytical modeling and formulation of the problem being provided in the second section, while the numerical results and discussion and concluding remarks are given in the sections three and four, respectively.

2. Analytical Formulation

In the present research work, the influence of parametric properties, i.e., chemical potential (μ), scattering rate (τ), slab thickness (d), and temperature (T) using dispersion relation, has been analyzed. The propagation of electromagnetic surface waves which travel along the interface of two media of different dielectric constants (i.e., graphene and indium antimonide) is studied. These waves are also known as surface plasmon polariton (SPP) which decays exponentially as the distance from the interface increases. There are three regions which are shown in Figure 1, upper region ($z > d$) which is free space, the middle region is supposed to filled with the indium antimonide (InSb), i.e., $0 < z < d$ and the at $z = d$ is the interface between the graphene layer and indium antimonide has been considered, while the lower region ($z < 0$) whose electrical conductivity is infinite.

To physically model such planar integrated structures, the different approaches, i.e., Dyadic green's function approach [39], effective medium approach [40], transmission line approach [41], equivalent circuit model approach [42], and analytic absorber model approach [43], have been used in the literature. However, in the present work, the waveguide approach has been used to model the supporting electromagnetic field interaction and propagation of the surface waves supported by the proposed structure, and the proposed approach is quite simple and easy to handle as reported in different works [10, 44].

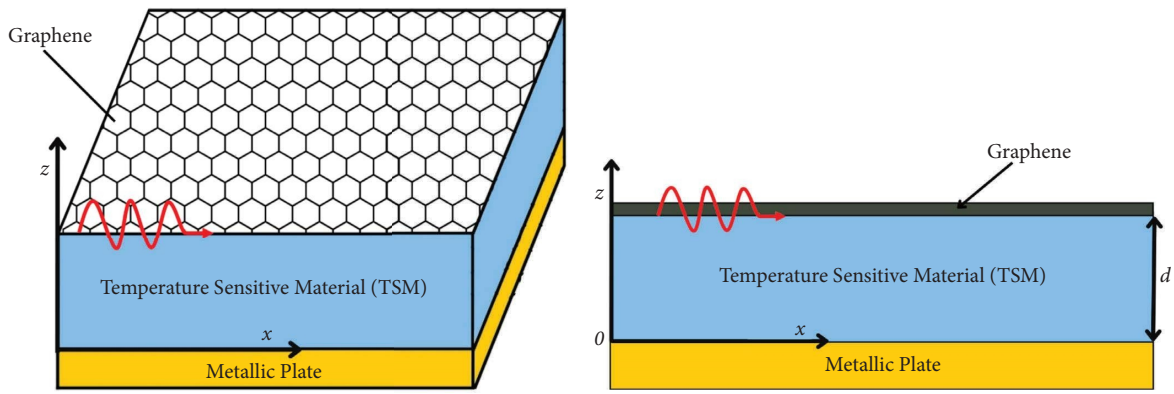

FIGURE 1: Geometry for surface waves supported by graphene-loaded InSb planar structure: (a) top view; (b) side view.

2.1. TM-Polarized Surface Waves. For transverse magnetic polarized surface waves, the electric field (E) is directed along the interface such as in the x-axis and the magnetic field (H) is directed along the y-axis. The associated field equations are as follows [11, 44].

For region $z > d$,

$$H_y^{(1)} = \mathrm{A}e^{-i\beta x}e^{-\gamma_1 z}, \tag{1}$$

$$E_x^{(1)} = -\frac{1}{i\omega\epsilon_o}\gamma_1 \mathrm{A}e^{-i\beta x}e^{-\gamma_1 z}. \tag{2}$$

For region $0 < z < d$,

$$H_y^{(2)} = \mathrm{B}e^{-i\beta x}\cos h\gamma_2 z, \tag{3}$$

$$E_x^{(2)} = -\frac{1}{i\omega\epsilon}\gamma_2 \mathrm{B}e^{-i\beta x}\sin h\gamma_2 z, \tag{4}$$

where $\gamma_1 = \sqrt{\beta^2 - \omega^2\mu_o\epsilon_o}$ and $\gamma_2 = \sqrt{\beta^2 - \omega^2\mu\epsilon}$ are attenuation constants for their respective regions, while A and B are unknown coefficients, $e^{-\gamma_1 z}$ is the exponential decay or damping, ω is the Terahertz radiation frequency, and β is known as the propagation constant. To calculate the unknown constants for the transverse magnetic surface waves, the boundary conditions are applied at $z = d$. Boundary conditions are given as [27]

$$H_y^{(1)} - H_y^{(2)} = J_s = \sigma_g E_x^{(2)}, \tag{5}$$

$$E_x^{(1)} - E_x^{(2)} = 0. \tag{6}$$

By implementing boundary conditions on (1)–(6), the characteristic equation for TM-polarized surface wave is obtained as

$$\frac{\epsilon}{\epsilon_o} + \frac{\gamma_2}{\gamma_1}\tan h\gamma_2 d + \frac{\sigma_g\gamma_2}{i\omega\epsilon_o}\tan h\gamma_2 d = 0. \tag{7}$$

2.2. TE-Polarized Surface Waves. For transverse electric polarized surface waves, the field equations are as the propagation of surface waves in which the electric field (E) is taken along y-axis and the magnetic field (H) is directed along x-axis, known as transverse electric TE-polarized surface waves [11, 44].

For region $z > d$,

$$E_y^{(1)} = \mathrm{A}e^{-i\beta x}e^{-\gamma_1 z}, \tag{8}$$

$$H_x^{(1)} = -\frac{1}{i\omega\mu_o}\gamma_1 \mathrm{A}e^{-i\beta x}e^{-\gamma_1 z}. \tag{9}$$

For region $0 < z < d$,

$$E_y^{(2)} = \mathrm{B}e^{-i\beta x}\sin h\gamma_2 z, \tag{10}$$

$$H_x^{(2)} = \frac{1}{i\omega\mu}\gamma_2 \mathrm{B}e^{-i\beta x}\cos h\gamma_2 z. \tag{11}$$

To calculate the unknown constants (A&B) for the transverse magnetic surface waves, the boundary conditions are applied at $z = d$. Boundary conditions are given as

$$H_x^{(1)} - H_x^{(2)} = J_s = \sigma_g E_y^{(2)}, \tag{12}$$

$$E_y^{(1)} - E_y^{(2)} = 0. \tag{13}$$

By implementing boundary conditions on (8)–(13), the characteristic equation for the TE-polarized surface wave is obtained as

$$\frac{\mu}{\mu_o} + \frac{\gamma_2}{\gamma_1}\cot h\gamma_2 d + \sigma_g\frac{i\omega\mu}{\gamma_1} = 0. \tag{14}$$

3. Numerical Results and Discussion

The wave properties of surface waves on graphene-loaded indium antimonide (InSb), i.e., dispersion relation, effective mode index, penetration depth, propagation length, phase velocity, and field profile, have been computed numerically. The characteristics of surface waves under the temperature, thickness of the InSb slab, and chemical potential variations have been studied. The numerical solution for each characteristic has been computed using the contour plot

technique. The scattering rate of electron-photon has been taken as $\tau = 0.6\,\text{ps}$. The modeling of graphene monolayer has been carried out [44, 45], using wolfram language-based Mathematica software. The electromagnetic modeling of graphene has been derived using Kubo's formalism. The optical surface conductivity of graphene is the result of the contribution of two factors, intraband and interband conduction [46]. The intraband conductivity supports graphene as a strong candidature for the tunability of surface waves in the Terahertz regime. It is caused by electron-photon processes. The intraband conductivity [46] is given as

$$\sigma_{\text{intraband}} = i\frac{e^2 K_B T}{\pi * \hbar^2 (\omega + i/\tau)}\left(\frac{\mu}{K_B T} + 2\ln\left[e^{-\mu/K_B T} + 1\right]\right), \quad (15)$$

whereas the interband conductivity facilitates graphene as a potential candidate for the tunability of surface waves in the visible and infrared regime. It is caused by direct electron interband transitions. The interband conductivity term [46] is given as

$$\sigma_{\text{interband}} = i\frac{e^2}{4\pi\hbar}\ln\left(\frac{2|\mu| - h(\omega + i/\tau)}{2|\mu| + h(\omega + i/\tau)}\right). \quad (16)$$

The interband conductivity dominates at THz and infrared frequencies, and graphene gives constant conductivity which is given as $\sigma_{\text{interband}} = e^2/4\hbar$. It means that a monolayer graphene sheet can absorb 2.3% of the incident light over a large frequency gap [47]. The total conductivity of graphene can be taken as the sum of intraband and interband conduction, i.e., $\sigma_g = \sigma_{\text{intraband}} + \sigma_{\text{interband}}$.

$$\sigma_g = i\frac{e^2 k_B T}{\pi * \hbar^2 (\omega + i/\tau)}\left(\frac{\mu}{k_B T} + 2\ln\left[\exp^{-\mu/k_B T} + 1\right]\right) + i\frac{e^2}{4\pi\hbar}\ln\left(\frac{2|\mu| - h(\omega + i/\tau)}{2|\mu| + h(\omega + i/\tau)}\right), \quad (17)$$

where the termsω, μ, T, k_B, $\hbar$, and τ stand for the incident frequency, chemical potential, temperature, Boltzmann constant, reduced Plank's constant, and electron-photon scattering rate, respectively.

3.1. Surface Waves on Graphene-Covered InSb. The effect of tuning the parameters, i.e., thickness, temperature, and chemical potentials on propagation of surface waves for graphene-covered indium antimonide slab, has been studied and calculated using Mathematica. The amplitude of surface waves decreases as we move away from the indium antimonide slab. With respect to polarization, two types of modes can be discussed for such types of surface waves which are given as

(i) TE-polarized surface wave

(ii) TM-polarized surface wave

Figure 2 shows the dispersion curves of TE-polarized surface waves with the variation of temperature, i.e., $T = 200\,\text{K}$, $T = 220\,\text{K}$, $T = 240\,\text{K}$, $T = 260\,\text{K}$, $T = 280\,\text{K}$, and $T = 300\,\text{K}$. It is predicted that the TE mode for such type of surface waves facilitated by graphene and indium antimonide structure does not exist since no variation in the straight line has been found on the tuning of temperature. All the lines obtained at various temperature variations follow a light line. So, there exists no solution for such temperature variations. Therefore, it is concluded that TE mode for electromagnetic surface waves does not exist unlike TM mode, which is consistent with the literature as given in [10, 44], while in the subsequent section, the numerical results for the surface wave under TM mode have been given.

3.2. Dispersion Curve Analysis for TM Polarization. In this section, propagation of the transverse magnetic polarized surface for indium antimonide and graphene-coated indium antimonide has been studied graphically and calculated using software pack. The electromagnetic modeling of temperature-sensitive materials such as indium antimonide can be tunable by controlling the temperature values. For Terahertz regime, the relative permittivity of InSb is given by the Drude model [44, 48].

$$\varepsilon_{\text{InSb}} = \varepsilon_\infty - \frac{\omega_p^2}{\omega^2 + i\gamma\omega}. \quad (18)$$

Herein, ε_∞ is the high frequency relative permittivity, ω_p is the plasma frequency, and γ is the damping constant. Plasma frequency ω_p can be calculated as $\omega_p = \sqrt{Nq_e/0.015\,\varepsilon_{o m_e}}$; here, the plasma frequency (ω_p) is affected by the intrinsic carrier density "N," electronic charge "q_e," and mass of electron "m_e", i.e., $q_e = -1.6 \times 10^{-19}\,C$, $m_e = 9.1 \times 10^{-31}\,\text{kg}$, and $\gamma = \pi \times 10^{11}\,\text{rad}\,s^{-1}$. The intrinsic carrier density "N" depends upon the temperature "T," bandgap "E_g," and Boltzmann constant "k_B" and can be calculated as $N = 5.76 \times 10^{20}\,T^{3/2}\exp\,(-E_g/2k_B T)$ where the values of band gap "E_g" and Boltzmann constant "k_B" are $0.26\,\text{eV}$ and $8.62 \times 10^{-5}\,\text{eV}/K$. As intrinsic carrier density "N" depends upon the temperature "T," we can say that the plasma frequency is also dependent upon the temperature. Therefore, by tuning the temperature of indium antimonide (InSb), the plasma frequency can be adjusted. Thus, the relative permittivity of InSb can be controlled in Figure 3 by varying the temperature parameters.

The dispersion curves of TM-polarized surface waves supported by graphene-loaded InSb under the variation of temperature, chemical potential, and thickness of InSb slab have been presented graphically in Figure 4. Figure 4(a) depicts that with the increase in temperature, high resonance frequency-polarized surface waves on an InSb slab coated

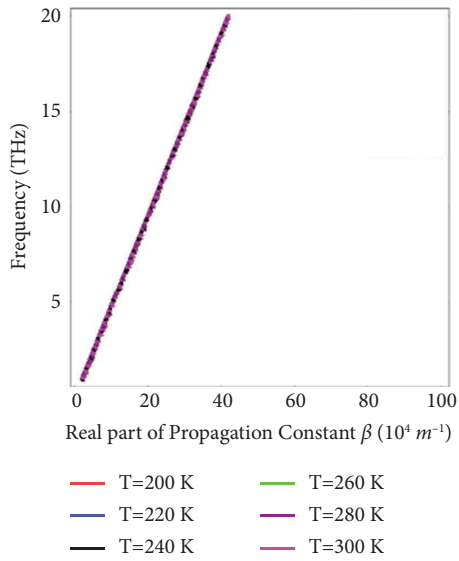

FIGURE 2: Influence of temperature on the dispersion curve for the TE-polarized surface wave propagation supported by graphene-coated indium antimonide with $\epsilon_\infty = 15.68$ and $\mu = 0.2$ eV.

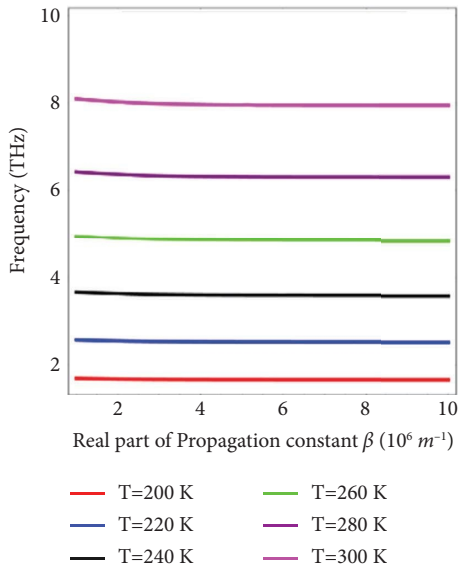

FIGURE 3: Dispersion curve analysis under the influence of temperature for the TM-polarized surface wave propagation supported by indium antimonide (InSb) with $\epsilon_\infty = 15.68$.

with graphene can be achieved. The impact of chemical potential on the dispersion curve by keeping the temperature constant has been presented in Figure 4(b). It has been found that with the increase of chemical potential, i.e., 0.2 eV, 0.4 eV, 0.6 eV, and 0.8 eV, the resonance frequency decreases. It is obvious from the figure that the chemical potential (μ) affects the conductivity of graphene and the propagation constant starts decreasing with the increase of chemical potential, which shows that for the highly doped graphene layer, the confinement of the surface waves is low. Further, it can be deduced from this result that the skin depth of THz for graphene-coated InSb slab starts decreasing. Due to this reason, the confinement of the surface wave also decreases with the increase of chemical potential. While the effects of the thickness of InSb slab on the propagation of surface waves supported by graphene-coated InSb slab have been depicted in Figure 4(c), it is clear from the figure that with the increase in the thickness d of the InSb slab, the resonance frequency decreases rapidly even at low THz frequency.

The ratio of the propagation constant of medium to free space is known as the effective mode index N_{eff}. The normalized effective wave number determines how surface waves are being confined at the interface and calculated as $N_{\text{eff}} = \text{Re}\,\beta/k_o$. On the graphene-coated THz-InSb slab, the confinement of the TM-polarized surface waves has been reported under temperature range, i.e., $T = 200$ K, 250 K, 300 K, 350 K, and 400 K in Figure 5. It is clear from the figure that with increasing temperature, the effective wave number of transverse magnetic-polarized surface waves also increases. Resultantly, the confinement of such surface waves supported by graphene-loaded indium antimonide THz slab also increases.

To further study the confinement of the surface waves on the graphene supported THz-InSb slab, the influence of thickness of InSb slab on the effective mode index (N_{eff}) under the function of frequency has been explained graphically in Figure 6. The possible solution has been calculated using the contour plot technique. Higher values of effective mode index mean higher confinement. It is clear from the figure that thickness of the slab plays an important role in tuning the confinement of surface waves. The effective mode index under the different values of thickness, i.e., $d = 20$ nm, $d = 40$ nm, $d = 60$ nm, $d = 80$ nm, and $d = 100$ nm, has been analyzed. It is obvious from the figure that with the increase of thickness of the InSb slab, the effective mode index decreases, and consequently, the confinement of such waves decreases from higher THz frequencies. Figure 7.

Propagation length (L_p) is the measurement of the distance travelled by a surface wave while travelling along the interface of two media and is given by the imaginary part of the propagation constant. The effect of temperature on the propagation length has been presented in Figure 8. The propagation length is normalized by wave number k_o. It depicts that propagation length increases with the increase in frequency. It is also concluded that with the increase in temperature, it shifts towards a high-frequency range.

In Figure 9, the influence of temperature on the phase velocity has been shown graphically. Phase velocity is given as $V_p = k_o/\beta$. To estimate the phase velocity within the temperature range of $T = 200$ K to 400 K, it is evident from Figure 9 that the phase velocity decreases as the frequency increases and can be adjusted by varying the temperature.

The comparison among the field profile of electromagnetic surface waves under different temperatures, i.e., $T = 200$ K and $T = 400$ K, has been presented in Figure 10. The normalized field profiles of $|E_x|$ have been taken as a function of transverse distance (z) from the interface. It is obvious from the figure that the field profiles are temperature-sensitive; i.e., high temperature has more intensity as compared to lower temperature.

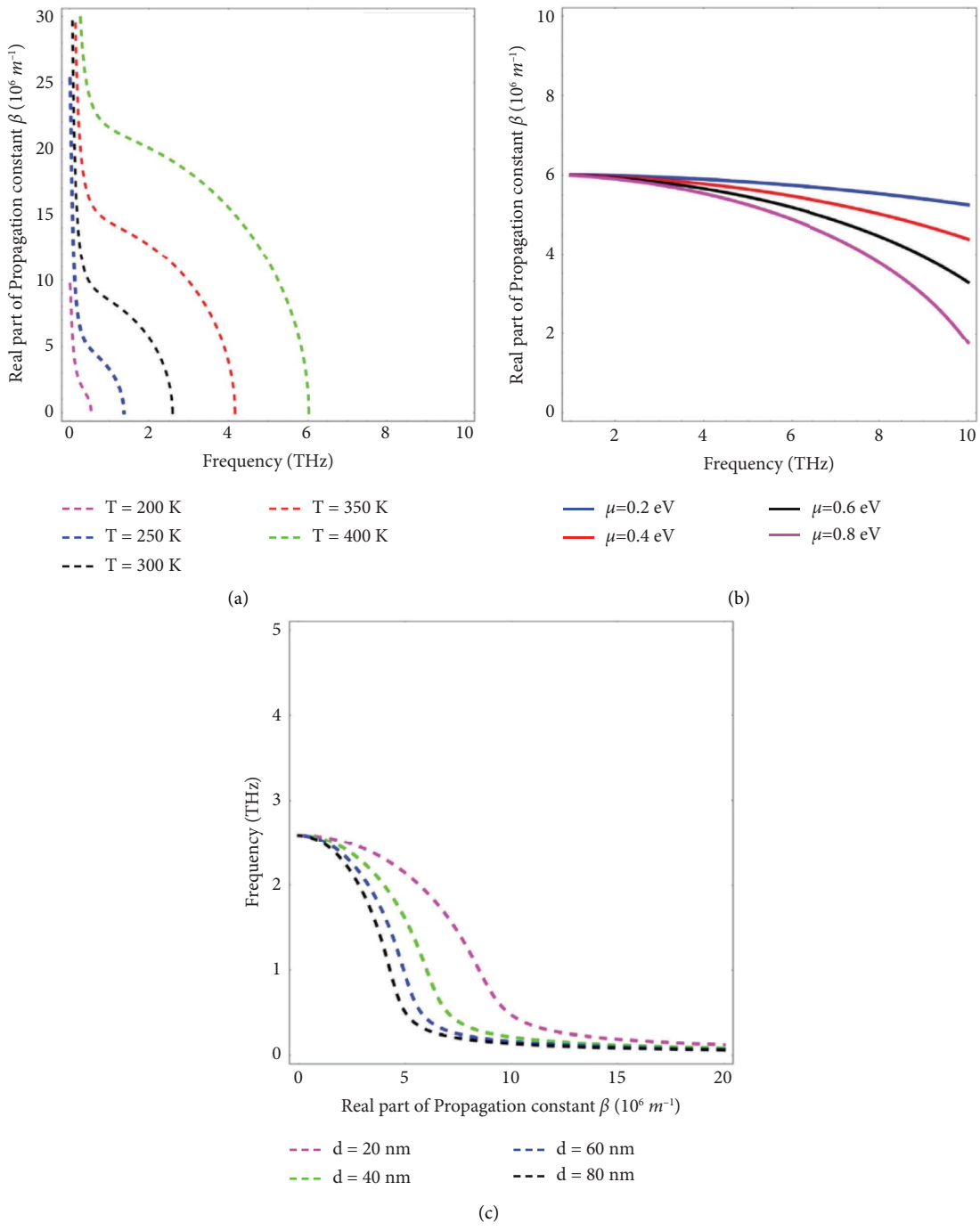

FIGURE 4: Dispersion curve analysis for the TM surface wave propagation supported by graphene-coated InSb (a) under the variation of temperature at $\epsilon_\infty = 15.68, \mu = 0.2\,\text{eV}$, and $d = 20\,\text{nm}$, (b) under the variation of chemical potential (μ), $\epsilon_\infty = 15.68, T = 300\,\text{K}$, and $d = 20\,\text{nm}$, and (c) under the variation of thickness with parameters $\epsilon_\infty = 15.68, T = 300\,\text{K}$, $d = 20\,\text{nm}$, and $\mu = 0.2\,\text{eV}$.

Further, it can be verified from the figure that as the transverse distance from the interface increases, the field profiles follow the exponential decay, which confirms the basic characteristic of surface waves.

In view of the practical implementation, the proposed structure can be easily realizable. The synthesis of graphene can be carried out by the chemical vapor deposition on the indium antimonide substrate [44]; however, the major limitation is the excitation scheme for the surface waves in the THz regime, and to bridge this limitation, many approaches have been studied for the excitation of such evanescent modes in THz, which may be used for the realization of the work [49]. The proposed results have potential applications in the designing of the temperature-assisted THz optical devices for the communication, thermal imaging, and sensing applications.

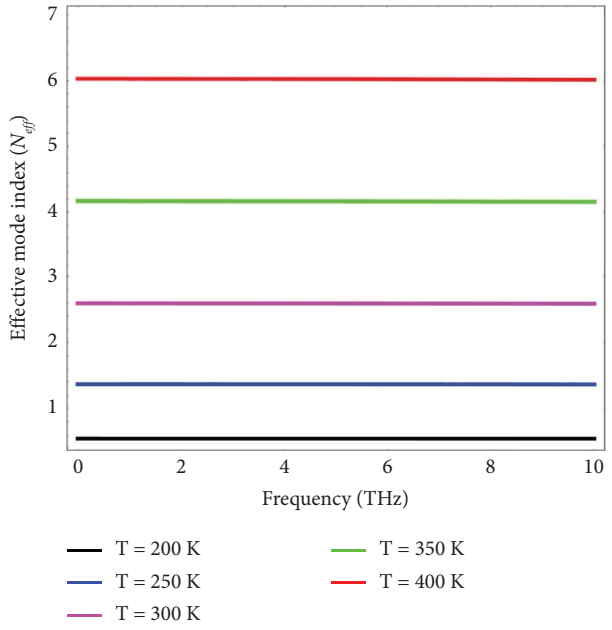

FIGURE 5: Influence of temperature on the effective mode index N_{eff} for the TM-polarized surface wave propagation assisted by graphene-coated indium antimonide with parameters $\epsilon_\infty = 15.68$, $d = 20$ nm and $\mu = 0.2$ eV.

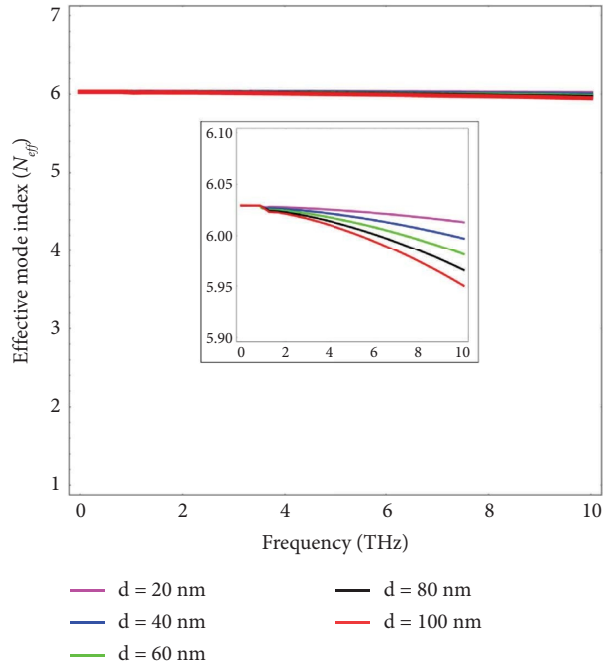

FIGURE 6: Effective mode index N_{eff} versus frequency under the variation of thickness for the TM-polarized surface wave propagation assisted by graphene-coated indium antimonide (InSb) with $\epsilon_\infty = 15.68$, $T = 400$ K, and $\mu = 0.2$ eV.

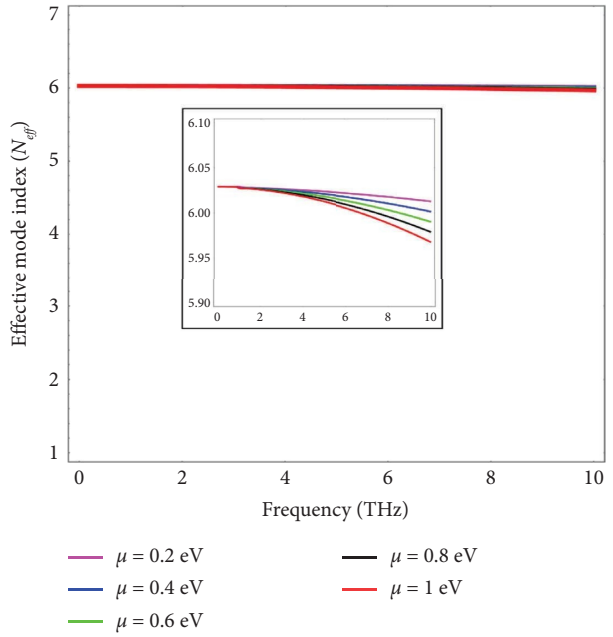

FIGURE 7: Influence of chemical potential μ on the effective mode index N_{eff} for the TM-polarized surface wave propagation supported by graphene-coated indium antimonide with $\epsilon_\infty = 15.68$, $d = 20$ nm, and $T = 400$ K.

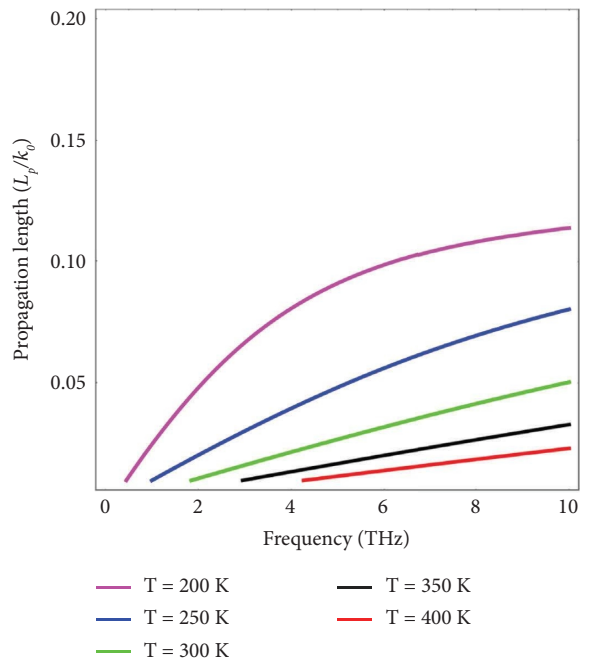

FIGURE 8: Influence of temperature on the propagation length (L_{p}) versus frequency (ω) on for the TM-polarized surface wave propagation assisted by graphene-coated indium antimonide (InSb) with $\epsilon_\infty = 15.68$, $d = 20$ nm, and $\mu = 0.8$ eV.

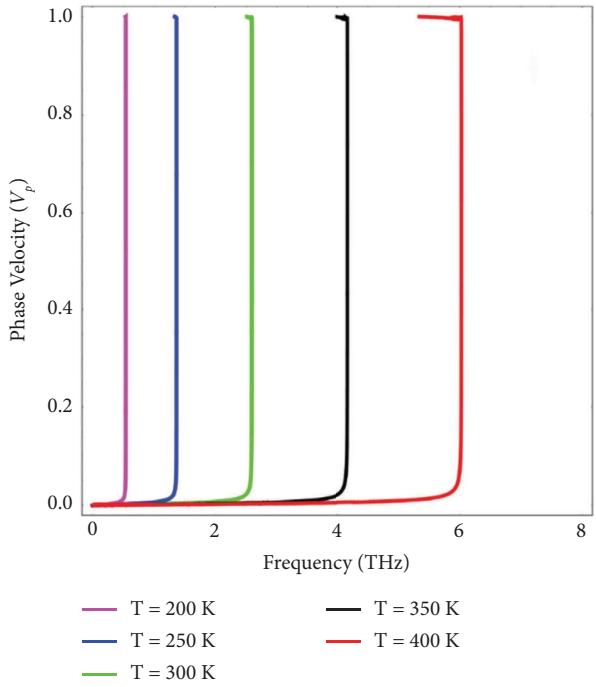

FIGURE 9: Phase velocity (V_p) under the variation of temperature on the surface wave propagation supported by graphene-coated indium antimonide with $\epsilon_\infty = 15.68$, $d = 20$ nm, and $\mu = 0.2$ eV.

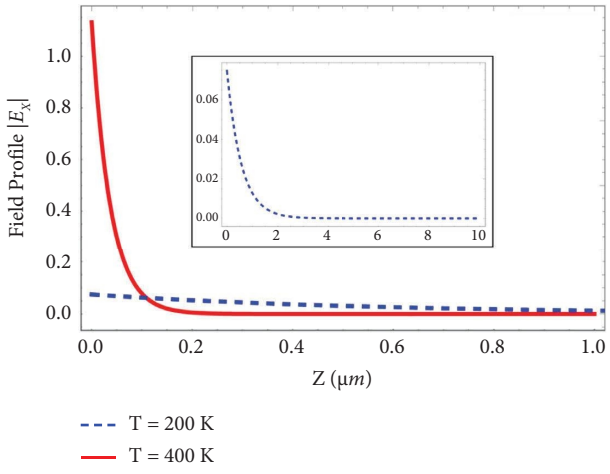

FIGURE 10: Comparison of field profiles for the TM-polarized surface waves propagating on the graphene-coated indium antimonide under different temperatures, i.e., $T = 200$ K (dashed blue line) with parameters $f = 0.354$ THz, $\beta = 1.765 \times 10^6$ m^{-1}, $\epsilon_\infty = 15.68$, $d = 20$ nm, and $\mu = 0.2$ eV and $T = 400$ K (thick red line) with parameters $f = 0.354$ THz, $\beta = 26.73 \times 10^6$ m^{-1}, $\epsilon_\infty = 15.68$, $d = 20$ nm, and $\mu = 0.2$ eV.

4. Concluding Remarks

The electromagnetic surface wave propagation supported by graphene-coated indium antimonide (InSb) has been studied in detail. Maxwell's equations have been solved using surface waves propagating on graphene supported by temperature-sensitive materials, such as indium antimonide, for transverse electric (TE) and transverse magnetic (TM) modes of polarization. Analytical and numerical studies have been conducted on the electromagnetic surface wave propagation on graphene coated with indium antimonide. For mathematical and graphical analysis, the Wolfram Mathematica pack has been utilized. The subsequent conclusions from the numerical results can be derived as the electromagnetic surface waves exit for only TM polarization, while in the case of TE polarization, there is no existence of surface waves. The propagation characteristics of surface waves are found to be temperature-sensitive. The propagation length, penetration depth, effective mode index, and phase velocity of surface waves can be varied by tuning the temperature. It is observed that the resonance frequency of surface waves is found to increase with temperature. The confinement of the surface waves can be tuned by the operating frequency and temperature of InSb. The field profile of the surface wave decreases progressively and decreases as the distance from the interface increases. The proposed results can be used for the realization and future application of the graphene-coated TSM structure for Terahertz applications in designing thermo-optical sensing, THz communication, and near-field thermal imaging platforms. Moreover, the work can be extended for the graphene-based curvilinear temperature-sensitive metasurfaces and bilayer asymmetric temperature-sensitive surfaces for the flexible thermo-optical sensors in THz regime as discussed in [50, 51].

Data Availability

The data used to support the findings of this study are included in the article.

Conflicts of Interest

The authors declare that they have no conflicts of interest.

Acknowledgments

This work was supported by the researchers supporting project number RSP2024R416, King Saud University, Riyadh, Saudi Arabia.

References

[1] M. Shinn and W. Robertson, "Surface plasmon-like sensor based on surface electromagnetic waves in a photonic band-gap material," *Sensors and Actuators B: Chemical*, vol. 105, no. 2, pp. 360–364, 2005.

[2] V. N. Konopsky and E. V. Alieva, "Photonic crystal surface waves for optical biosensors," *Analytical Chemistry*, vol. 79, no. 12, pp. 4729–4735, 2007.

[3] I. Abdulhalim, M. Zourob, and A. Lakhtakia, "Surface plasmon resonance for biosensing: a mini-review," *Electromagnetics*, vol. 28, no. 3, pp. 214–242, 2008.

[4] J. S. Sekhon and S. Verma, "Plasmonics: the future wave of communication," *Current Science*, vol. 101, no. 4, pp. 484–488, 2011.

[5] O. Takayama, D. Artigas, and L. Torner, "Practical dyakonons," *Optics Letters*, vol. 37, no. 20, pp. 4311–4313, 2012.

[6] V. E. Ferry, L. A. Sweatlock, D. Pacifici, and H. A. Atwater, "Plasmonic nanostructure design for efficient light coupling into solar cells," *Nano Letters*, vol. 8, no. 12, pp. 4391–4397, 2008.

[7] L. Liu, G. D. Barber, M. V. Shuba et al., "Planar light concentration in micro-Si solar cells enabled by a metallic grating–photonic crystal architecture," *ACS Photonics*, vol. 3, no. 4, pp. 604–610, 2016.

[8] J. A. Polo Jr and A. Lakhtakia, "Surface electromagnetic waves: a review," *Laser and Photonics Reviews*, vol. 5, no. 2, pp. 234–246, 2011.

[9] J. Pitarke, V. Silkin, E. Chulkov, and P. Echenique, "Theory of surface plasmons and surface-plasmon polaritons," *Reports on Progress in Physics*, vol. 70, no. 1, pp. 1–87, 2006.

[10] S. A. Maier, *Plasmonics: Fundamentals and Applications*, vol. 1, Springer, Berlin, Germay, 2007.

[11] J. Polo, T. Mackay, and A. Lakhtakia, *Electromagnetic Surface Waves: A Modern Perspective*, Newnes, Oxford, UK, 2013.

[12] J. Zenneck, "The propagation of plane electro-magnetic waves over a flat earth and its application to wireless telegraphy," *Annalen der Physik*, vol. 23, p. 846, 1907.

[13] R. E. Collin, "Hertzian dipole radating over a lossy earth or sea: some early and late 20th-century controversies," *IEEE Antennas and Propagation Magazine*, vol. 46, no. 2, pp. 64–79, 2004.

[14] K. Corum, J. Corum, and M. Miller, "Surface waves and the 'crucial'propagation experiment—the key to efficient wireless power delivery," in *Proceedings of the 2016 Texas Symposium on Wireless and Microwave Circuits and Systems (WMCS)*, IEEE, Waco, TX, USA, March, 2016.

[15] C. Qiu, Y.-B. Wang, Y.-Y. Chen, Y.-X. Lei, L. Qin, and L.-J. Wang, "Design and analysis of a novel graphene-assisted silica/polymer hybrid waveguide with thermal–optical phase modulation structure," *IEEE Photonics Journal*, vol. 11, no. 2, pp. 1–10, 2019.

[16] N. Mohammadi Estakhri, B. Edwards, and N. J. S. Engheta, "Inverse-designed metastructures that solve equations," *Science*, vol. 363, no. 6433, pp. 1333–1338, 2019.

[17] L. La Spada and L. J. O. E. Vegni, "Near-zero-index wires," *Optics Express*, vol. 25, no. 20, pp. 23699–23708, 2017.

[18] Z. Lalegani, S. S. Ebrahimi, B. Hamawandi, L. La Spada, H. Batili, and M. J. M. C. Toprak, "Targeted dielectric coating of silver nanoparticles with silica to manipulate optical properties for metasurface applications," *Materials Chemistry and Physics*, vol. 287, Article ID 126250, 2022.

[19] M. B. Heydari and M. H. V. Samiei, "Plasmonic graphene waveguides: a literature review," 2018, https://arxiv.org/ftp/arxiv/papers/1809/1809.09937.pdf.

[20] J. N. Anker, W. P. Hall, O. Lyandres, N. C. Shah, J. Zhao, and R. P. Van Duyne, "Biosensing with plasmonic nanosensors," *Nature Materials*, vol. 7, no. 6, pp. 442–453, 2008.

[21] N. J. Greybush, V. Pacheco-Peña, N. Engheta, C. B. Murray, and C. R. J. A. N. Kagan, "Plasmonic optical and chiroptical response of self-assembled Au nanorod equilateral trimers," *ACS Nano*, vol. 13, no. 2, pp. 1617–1624, 2019.

[22] D. T. Nurrohman and N.-F. J. N. Chiu, "A review of graphene-based surface plasmon resonance and surface-enhanced Raman scattering biosensors: current status and future prospects," *Nanomaterials*, vol. 11, no. 1, p. 216, 2021.

[23] M. Saeed, A. Ghaffar, S. U. Rehman, M. Y. Naz, S. Shukrullah, and Q. A. J. P. Naqvi, "Graphene-based plasmonic waveguides: a mini review," *Plasmonics*, vol. 17, no. 3, pp. 901–911, 2022.

[24] M. Akbari, M. J. Shahbazzadeh, L. La Spada, and A. J. A. S. Khajehzadeh, "The graphene field effect transistor modeling based on an optimized ambipolar virtual source model for DNA detection," *Applied Sciences*, vol. 11, no. 17, p. 8114, 2021.

[25] L. Wang, A. Wu, and G. J. A. Wei, "Graphene-based aptasensors: from molecule–interface interactions to sensor design and biomedical diagnostics," *The Analyst*, vol. 143, no. 7, pp. 1526–1543, 2018.

[26] A. Vakil and N. Engheta, "Manipulating IR surface plasmon polaritons on graphene," in *Frontiers in Optics*, Optica Publishing Group, Washington, DC, USA, 2010.

[27] A. Vakil and N. Engheta, "Transformation optics using graphene," *Science*, vol. 332, no. 6035, pp. 1291–1294, 2011.

[28] M. Naserpour, C. J. Zapata-Rodríguez, S. M. Vuković, H. Pashaeiadl, and M. R. Belić, "Tunable invisibility cloaking by using isolated graphene-coated nanowires and dimers," *Scientific Reports*, vol. 7, no. 1, Article ID 12186, 2017.

[29] S.-H. Lee, J.-H. Choe, C. Kim et al., "Graphene assisted terahertz metamaterials for sensitive bio-sensing," *Sensors and Actuators B: Chemical*, vol. 310, Article ID 127841, 2020.

[30] M. Shimatani, S. Ogawa, S. Fukushima, S. Okuda, K. Inoue, and K. Matsumoto, "Multispectral graphene infrared photodetectors using plasmonic metasurfaces," in *Infrared Technology and Applications XLV*, SPIE, Washington, DC, USA, 2019.

[31] H. P. Adl, S. Gorji, M. K. Habil et al., "Purcell enhancement and wavelength shift of emitted light by CsPbI3 perovskite nanocrystals coupled to hyperbolic metamaterials," *ACS Photonics*, vol. 7, no. 11, pp. 3152–3160, 2020.

[32] F. De Nicola, N. S. Puthiya Purayil, V. Miŝeikis et al., "Graphene plasmonic fractal metamaterials for broadband photodetectors," *Scientific Reports*, vol. 10, no. 1, p. 6882, 2020.

[33] A. Nag, R. B. Simorangkir, D. R. Gawade et al., "Graphene-based wearable temperature sensors: a review," *Materials and Design*, vol. 221, Article ID 110971, 2022.

[34] M. Kang, H. Jeong, S.-W. Park et al., "Wireless graphene-based thermal patch for obtaining temperature distribution and performing thermography," *Science Advances*, vol. 8, no. 15, Article ID eabm6693, 2022.

[35] S. Chen, K. Jiang, Z. Lou, D. Chen, and G. J. A. M. T. Shen, "Recent developments in graphene-based tactile sensors and E-skins," *Advanced Materials Technologies*, vol. 3, no. 2, Article ID 1700248, 2018.

[36] M. Wuttig, H. Bhaskaran, and T. J. N. P. Taubner, "Phase-change materials for non-volatile photonic applications," *Nature Photonics*, vol. 11, no. 8, pp. 465–476, 2017.

[37] H. Liu, G. Ren, Y. Gao, Y. Lian, Y. Qi, and S. Jian, "Tunable subwavelength terahertz plasmon-induced transparency in the InSb slot waveguide side-coupled with two stub resonators," *Applied Optics*, vol. 54, no. 13, pp. 3918–3924, 2015.

[38] A. Moazami, M. Hashemi, and N. C. Shirazi, "High efficiency tunable graphene-based plasmonic filter in the THz frequency range," *Plasmonics*, vol. 14, no. 2, pp. 359–363, 2019.

[39] L. Vegni, R. Cicchetti, and P. Capece, "Spectral dyadic Green's function formulation for planar integrated structures," *IEEE Transactions on Antennas and Propagation*, vol. 36, no. 8, pp. 1057–1065, 1988.

[40] V. Pacheco-Peña, N. Engheta, S. Kuznetsov, A. Gentselev, and M. Beruete, "All-metallic epsilon-near-zero graded-index converging lens at terahertz frequencies," in *Proceedings of the 12th European Conference on Antennas and Propagation (EuCAP 2018)*, IET, London, UK, April, 2018.

[41] V. Pacheco-Peña, M. Beruete, P. Rodríguez-Ulibarri, and N. J. N. J. O. P. Engheta, "On the performance of an ENZ-based sensor using transmission line theory and effective medium approach," *New Journal of Physics*, vol. 21, no. 4, Article ID 043056, 2019.

[42] L. J. S. La Spada, "Metasurfaces for advanced sensing and diagnostics," *Sensors*, vol. 19, no. 2, p. 355, 2019.

[43] L. La Spada and L. J. O. E. Vegni, "Metamaterial-based wideband electromagnetic wave absorber," *Optics Express*, vol. 24, no. 6, pp. 5763–5772, 2016.

[44] M. Yaqoob, M. Ahamd, A. Ghaffar, F. Razzaz, S. Saeed, and T. M. Alanazi, "Thermally tunable electromagnetic surface waves supported by graphene loaded indium antimonide (InSb) interface," *Scientific Reports*, vol. 13, no. 1, Article ID 18631, 2023.

[45] M. Yaqoob, A. Ghaffar, M. A. Alkanhal, M. Naz, A. H. Alqahtani, and Y. Khan, "Tunable surface waves supported by graphene-covered left-handed material structures," *Optics Communications*, vol. 489, Article ID 126874, 2021.

[46] X. Luo, T. Qiu, W. Lu, and Z. Ni, "Plasmons in graphene: recent progress and applications," *Materials Science and Engineering: R: Reports*, vol. 74, no. 11, pp. 351–376, 2013.

[47] X. Gu, *Graphene-based Surface Plasmon-Polaritons for Terahertz Applications*, University of California, Los Angeles, CA, USA, 2013.

[48] J. Han and A. Lakhtakia, "Semiconductor split-ring resonators for thermally tunable terahertz metamaterials," *Journal of Modern Optics*, vol. 56, no. 4, pp. 554–557, 2009.

[49] X. Zhang, Q. Xu, L. Xia et al., "Terahertz surface plasmonic waves: a review," *Advanced Photonics*, vol. 2, no. 01, Article ID 014001, 2020.

[50] L. La Spada, C. Spooner, S. Haq, and Y. J. S. R. Hao, "Curvilinear metasurfaces for surface wave manipulation," *Scientific Reports*, vol. 9, no. 1, p. 3107, 2019.

[51] Z. Zhao, Z. Gu, H. Zhao, and W. J. O. M. E. Shi, "Dual terahertz slow light plateaus in bilayer asymmetric metasurfaces," *Optical Materials Express*, vol. 9, no. 4, pp. 1608–1619, 2019.